

A Framework for Analysis of Computational Imaging Systems: Role of Signal Prior, Sensor Noise and Multiplexing

Kaushik Mitra, *Member, IEEE*, Oliver S. Cossairt, *Member, IEEE*
and Ashok Veeraraghavan, *Member, IEEE*

Abstract—Over the last decade, a number of Computational Imaging (CI) systems have been proposed for tasks such as motion deblurring, defocus deblurring and multispectral imaging. These techniques increase the amount of light reaching the sensor via multiplexing and then undo the deleterious effects of multiplexing by appropriate reconstruction algorithms. Given the widespread appeal and the considerable enthusiasm generated by these techniques, a detailed performance analysis of the benefits conferred by this approach is important.

Unfortunately, a detailed analysis of CI has proven to be a challenging problem because performance depends equally on three components: (1) the optical multiplexing, (2) the noise characteristics of the sensor, and (3) the reconstruction algorithm which typically uses signal priors. A few recent papers [12], [49], [30] have performed analysis taking multiplexing and noise characteristics into account. However, analysis of CI systems under state-of-the-art reconstruction algorithms, most of which exploit signal prior models, has proven to be unwieldy. In this paper, we present a comprehensive analysis framework incorporating all three components.

In order to perform this analysis, we model the signal priors using a Gaussian Mixture Model (GMM). A GMM prior confers two unique characteristics. Firstly, GMM satisfies the universal approximation property which says that any prior density function can be approximated to any fidelity using a GMM with appropriate number of mixtures. Secondly, a GMM prior lends itself to analytical tractability allowing us to derive simple expressions for the ‘minimum mean square error’ (MMSE) which we use as a metric to characterize the performance of CI systems. We use our framework to analyze several previously proposed CI techniques (focal sweep, flutter shutter, parabolic exposure, etc.), giving conclusive answer to the question: ‘How much performance gain is due to use of a signal prior and how much is due to multiplexing?’ Our analysis also clearly shows that multiplexing provides significant performance gains above and beyond the gains obtained due to use of signal priors.

Index Terms—Computational imaging, Extended depth-of-field (EDOF), Motion deblurring, GMM

1 INTRODUCTION

Computational Imaging systems can be broadly categorized into two categories [44]: those designed either to add a new functionality or to increase performance relative to a conventional imaging system. A light field camera [45], [56], [32], [39] is an example of the former: it can be used to refocus or change perspective *after* images are

- K. Mitra and A. Veeraraghavan are with the Department of Electrical and Computer Engineering, Rice University, Houston, TX, 77025. E-mail: Kaushik.Mitra@rice.edu and vashok@rice.edu
- O. S. Cossairt is with the Department of Electrical Engineering and Computer Science, Northwestern University, Evanston, IL 60208. E-mail: ollie@eecs.northwestern.edu

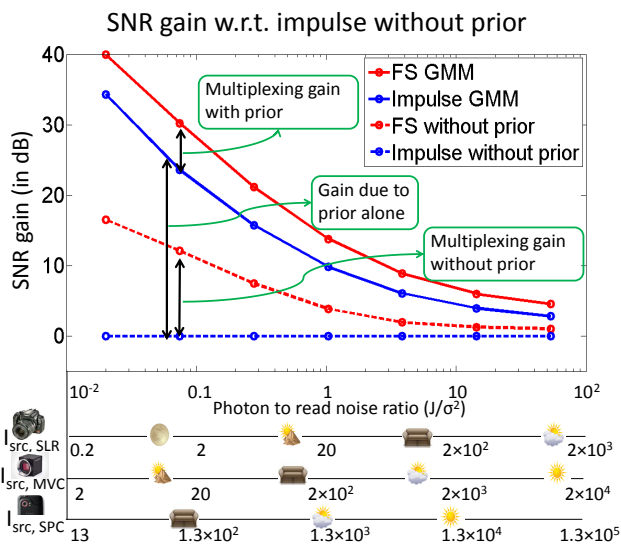


Fig. 1. *Effect of signal prior on multiplexing gain of focal sweep [31]:* We show the multiplexing gain of focal sweep over impulse imaging (a conventional camera with stopped down aperture) at different photon to read noise ratios J/σ_r^2 . The photon to read noise ratio is related to illumination level and camera specifications. In the extended x-axis, corresponding to different values of J/σ_r^2 , we show the light levels (in lux) for three camera types: a high end SLR, a machine vision camera (MVC) and a smartphone camera (SPC). As shown by Cossairt et al. [12], without using signal priors, we get a huge multiplexing gain at low J/σ_r^2 . However, given that most state-of-the-art reconstruction algorithms are based on signal priors, such huge gains are unrealistic. In practice, with the use of signal prior, we get much more modest gains. Our goal is to analyze the multiplexing gain of CI systems above and beyond the use of signal priors.

captured - a functionality impossible to achieve with a conventional camera. The latter type of systems are the focus of this paper, and from here on we use the term CI to refer to them. Examples include extended depth-of-

field (EDOF) systems [33], [56], [65], [27], [31], [16], [26], [35], [21], [7], [46], [20], [53], [64], motion deblurring [48], [38], [10], spectroscopy [24], [23], [58], color imaging [6], [30], multiplexed light field acquisition [56], [32], [39], [3], temporal multiplexing [57], [51], [28], [1], [29] and illumination multiplexing [52], [49]. These systems use optical coding (multiplexing) to increase light throughput, which increases the SNR of captured images. The desired signal is then recovered computationally via signal processing. The quality of recovered images depends jointly on the type of optical coding and the increased light throughput. A poor choice of multiplexing will reduce image quality.

The question of exactly how much performance improvement can be achieved via multiplexing has received a fair amount of attention in the literature [24], [11], [12], [30], [52], [60], [49], [26], [25]. It is well understood that multiplexing gives the greatest advantage at low light levels (where *signal-independent* read noise dominates), but this advantage diminishes with increasing light (where *signal-dependent* photon noise dominates) [24]. However, it is impractical to study the effects of multiplexing alone, since signal priors are at the heart of every state-of-the-art reconstruction algorithm (e.g. dictionary learning [4], BM3D [14], GMM [62], [43]). Signal priors can dramatically increase performance in problems of deblurring (multiplexed sensing) and denoising (no multiplexing), typically with greater improvement as noise increases (i.e. as the light level decreases). While both signal priors and multiplexing increase performance at low light levels, the former is trivial to incorporate and the latter often requires hardware modifications. Thus, it is imperative to understand the improvement due to multiplexing *beyond the use of signal priors*. However, comprehensive analysis of CI systems remains an elusive problem because state-of-the-art priors often use signal models unfavorable to analysis.

In this work, we follow a line of research whose goal is to derive bounds on the performance of CI systems [49], [30], and relate maximum performance to practical considerations (e.g. illumination conditions and sensor characteristics) [12]. We follow the convention adopted in [12], [49], [30], where the performance of the CI systems are compared against their corresponding *impulse imaging systems*, which are defined as a conventional camera that directly measures the desired signal (e.g. without blur). Noise is related to the lighting level, scene properties and sensor characteristics. In this paper, we pay special attention to the problems of defocus and motion blurs and to the problem of light field acquisition. Defocus and motion blurs can be position dependent when objects in the scene span either a range of depths or velocities. Various techniques have been devised to encode blur so as to make it either well-conditioned or position-independent (shift-invariant), or both. For defocus deblurring, CI systems encode defocus blur using attenuation masks [33], [56], [65], refractive masks [16], or motion [27], [31]. The impulse imaging counterpart is a narrow aperture image with no defocus blur. For motion deblurring, CI systems encode motion blur using a fluttered shutter [48] or camera motion [38], [10].

The impulse imaging counterpart is an image with short exposure time and no motion blur. Many camera designs have been proposed to capture light fields such as: the microlens array based light field camera (Lytro) [45], coded aperture camera [39], mask-near-sensor designs [56], [32] and camera array designs [59]. In this paper we analyze only single sensor, snapshot light field camera systems. The corresponding impulse camera, which directly captures the light field, is a pinhole array mask placed near the sensor.

Cossairt et al. [12] derived an upper bound stating that the maximum gain due to multiplexing is quite large at low light levels. For example, in Figure 1, the multiplexing gain of focal sweep is > 10 dB for a low photon to read noise ratio < 0.1 . However, as we show in this paper, this makes for an exceptionally weak bound because signal priors are not taken into account. In practice, signal priors can be used to improve the performance of any camera, impulse and computational alike. Since incorporating a signal prior can be done merely by applying an algorithm to captured images, it is natural to expect that we would always choose to do so. However, it has historically been very difficult to determine exactly how much of an increase in performance to expect from signal priors, making it difficult to provide a fair comparison between different cameras.

We present a comprehensive framework that allows us to analyze the performance of CI systems while simultaneously taking into account multiplexing, sensor noise, and signal priors. We characterize the performance of CI systems under a GMM prior which has two unique properties: Firstly, GMM satisfies the universal approximation property which says that any probability density function (with a finite number of discontinuities) can be approximated to any fidelity using a GMM with an appropriate number of mixtures [54], [47]. Secondly, a GMM prior lends itself to analytical tractability allowing us to derive simple expressions for the MMSE, which we use as a metric to characterize the performance of both impulse and computational imaging systems. We use our framework to analyze several previously proposed CI techniques (focal sweep, flutter shutter, parabolic exposure, etc.), giving conclusive answers to the questions: ‘How much gain is due to the use of a signal prior and how much is due to multiplexing? What is the multiplexing gain beyond the use of signal prior?’.

We show that the SNR benefits due to the use of a signal prior alone are quite large in low light and decrease as the light level increases (see Figure 1). Furthermore, show that when priors are taken into account, multiplexing provides us realistic gains of 9.6 dB for EDOF in low light conditions (see Figure 2), 7.5 dB for motion deblurring systems in low light conditions (see Figure 4), and 12 dB for light field systems in high light conditions (see Figure 6). These are substantial gains as these implies that the MSE of the CI systems are less than those of corresponding impulse systems by factors of 9, 5.5 and 16, respectively. This indicates that CI techniques improve the performance of traditional imaging beyond the benefits conferred due to sophisticated reconstruction algorithms.

1.1 Key Contributions

- 1) We introduce a framework for analysis of CI systems under signal priors. Our analysis is based on the GMM prior, which can approximate almost any probability density function and is analytically tractable.
- 2) We use the GMM prior to quantify exactly how much the use of signal priors can improve the performance of a given camera. We also quantify the multiplexing gain beyond that due to the use of signal priors.
- 3) We analyze the performance of many CI systems *with signal priors taken into account*. We show that the SNR gain due to multiplexing beyond the use of signal priors can be significant (9.6 dB for defocus deblurring cameras, 7.5 dB for motion deblurring systems, and 12 dB for light field systems).
- 4) We use the MMSE as a metric to characterize the performance of the impulse and CI systems. However, the MMSE under GMM prior can not be computed analytically. We show that for CI systems, an analytic lower bound on MMSE (derived in [19]) can very closely approximate the exact MMSE and can be used for analysis, see Figure 8.

1.2 Scope and Limitations

Image Formation Model. Our analysis assumes a linear image formation model. Non-linear imaging systems, such as a two/three photon microscopes and coherent imaging systems are outside the scope of this paper. Nevertheless, our analysis covers a very large array of existing imaging systems [48], [56], [33], [58], [30], [49]. We use a geometric optics model and ignore the effect of diffraction due to small apertures.

Noise Model. We use an affine noise model to describe the combined effects of *signal-independent* and *signal-dependent* noise. Signal-dependent Poisson noise is approximated using a Gaussian noise model (as described in Section 3.2).

Single Image Capture. We perform analysis of only single image CI techniques. Our results are therefore not applicable to multi-image capture techniques such as Hasinoff et al. [25] (EDOF), and Zhang et al. [63] (Motion Deblurring).

Patch Based Prior. Learning a GMM prior on entire images would require an impossibly large training set. To combat this problem, we train our GMM on image patches, and solve the image estimation problem in a patch-wise manner. As a result, our technique requires that multiplexed measurements are restricted to linear combinations of pixels in a neighborhood smaller than the GMM patch size.

Shift-Invariant Blur. We analyze motion and defocus deblurring cameras under the assumption of a single known shift-invariant blur kernel. This amounts to the assumption that either the depth/motion is position-independent, or the blur is independent of depth/motion. We do not analyze errors due to inaccurate kernel estimation (for coded aperture and flutter shutter [48], [56], [33]) or due to the degree of depth/motion invariance (for focal sweep, cubic phase plate, motion invariant photography [13], [5], [38], [10]).

2 RELATED WORK

Theoretical Analysis of CI systems: Harwit and Sloan [24] analyzed coded imaging systems and have shown that, in absence of photon noise, Hadamard and S-matrices are optimal. Wuttig and Ratner et al. [60], [49], [50] then extended the analysis to include both photon and read noise and showed that there is significant gain in multiplexing only when the read noise dominates over photon noise. Ihrke et al. [30] analyzed the performance of different light field cameras and color filter arrays. Tendero [55] has analyzed the performance of flutter shutter cameras with respect of impulse imaging (short exposure imaging). Agrawal and Raskar compared the performance of flutter shutter and motion invariant cameras [2]. Recently, Cossairt et al. [12], [11] has obtained optics independent upper bounds on performance for various CI techniques. However, all the above works, do not analyze the performance of CI systems when a signal prior is used for demultiplexing. Cossairt et al. [12] have performed empirical experiments to study the effect of priors, but conclusions drawn based from simulations are usually limited.

Performance Analysis using Image Priors: Zhou et al. [65] used a Gaussian signal prior and Gaussian noise model to search for good aperture codes for defocus deblurring. Levin et al. [34] have proposed the use of a GMM light field prior for comparing across different light field (LF) camera designs. They used the mean square error as a metric for comparing cameras. However, they do not take into account the effect of signal dependent noise.

Our approach is inspired in part by the recent analysis on the fundamental limits of image denoising [8], [36], [37], the only papers we are aware of that directly address the issue of performance bounds in the presence of image priors. Both of these recent results model image statistics through a patch based image prior and derive lower bounds on the MMSE for image denoising. We loosely follow the approach here and extend the analysis to general computational imaging systems. In order to render both computational tractability and generality, we use a GMM with a sufficient number of mixtures to model the prior distribution on image patches. Similar to [8], [36], [37], we then derive bounds and estimates for the MMSE and use these to analyze CI systems.

Practical Implications for CI systems: Cossairt et al. [12] analyzed CI systems based on application (e.g. defocus deblurring or motion deblurring), lighting condition (e.g. moonlit night or sunny day), scene properties (e.g. albedo, object velocity) and sensor characteristics (size of pixels). They have shown that, for commercial grade image sensors, CI techniques only improve performance significantly when the illumination is less than 125 lux (typical living room lighting). We extend these results to include the analysis of CI systems with signal priors taken into account. Hasinoff et al. [25] (in the context of EDOF) and Zhang et al. [63] (in the context of motion deblurring) analyzed the trade-off between denoising and deblurring for multi-shot imaging within a time budget. We analyzed the trade-off between denoising and deblurring for single shot capture.

3 PROBLEM DEFINITION AND NOTATION

We consider linear multiplexed imaging systems that can be represented as

$$y = Hx + n, \quad (1)$$

where $y \in R^N$ is the measurement vector, $x \in R^N$ is the unknown signal we want to capture, H is the $N \times N$ multiplexing matrix and n is the observation noise.

3.1 Multiplexing Matrix H

A large array of existing imaging systems follow a linear image formation model, such as flutter shutter [48], coded aperture [56], [33], [58], plenoptic multiplexing [30], illumination multiplexing [52], and many others. The results of this paper can be used to analyze all such systems. In this paper, we analyze motion and defocus deblurring systems and multiplexed light field systems. For motion and defocus blur, we concentrate mostly on systems that produce shift-invariant blur. For the case of 1D motion blur, the vectors x and y represent a scan line in a sharp and blurred image patch, respectively. The multiplexing matrix H is a Toeplitz matrix where the rows contain the system point spread function. For the case of 2D defocus blur, the vectors x and y represent lexicographically reordered image patches, and the multiplexing matrix H is block Toeplitz. For the case of light field systems, x and y represent lexicographically reordered light field and captured 2D multiplexed image patch and H matrix is a block Toeplitz matrix.

3.2 Noise Model

To enable tractable analysis, we use an affine noise model [52], [25]. We model signal independent noise as a Gaussian random variable with variance σ_r^2 . Signal dependent photon noise is Poisson distributed with parameter σ_p^2 equal to the average signal intensity at a pixel. We approximate photon noise by a Gaussian distribution with variance σ_p^2 . This is a good approximation when σ_p^2 is greater than 10. We also drop the pixel-wise dependence of photon noise and instead assume that the noise variance at every pixel is equal to the average signal intensity. For a given lighting and scene, if J is the average pixel value in the impulse camera, then the photon noise variance is given by $\sigma_p^2 = J$. For the same lighting and scene, the average pixel value for a CI camera (specified by multiplexing matrix H) is given by $C(H)J$, where $C(H)$ is the matrix light throughput, defined as the average row sum of H . Thus, the average photon noise variance for the CI system is $\sigma_p^2 = C(H)J$ and the overall noise model is given by:

$$f(n) = \mathcal{N}(0, C_{nn}), \quad C_{nn} = (\sigma_r^2 + C(H)J)\mathcal{I}, \quad (2)$$

where \mathcal{I} is the identity matrix with dimension equal to the number of observed pixels.

3.3 Signal Prior Model

In this paper, we choose to model scene priors using a GMM because of three characteristics:

- **State of the art performance:** GMM priors have provided state of the art results in various imaging applications such as image denoising, deblurring and superresolution [62], [22], still-image compressive sensing [62], [9], light field denoising and superresolution [43] and video compressive sensing [61]. GMM is also closely related to the union-of-subspace model [18], [17] as each Gaussian mixture covariance matrix defines a principle subspace.
- **Universal Approximation Property:** GMM satisfies the universal approximation property i.e., (almost) any prior can be approximated by learning a GMM with a large enough number of mixture components [54], [47]. To state this concisely, consider a family of zero mean Gaussian distributions $\mathcal{N}_\lambda(x)$ with variance λ . Let $p(x)$ be a prior probability density function with a finite number of discontinuities, that we want to approximate using a GMM distribution. Then the following Lemma holds:

Lemma 3.1: The sequence $p_\lambda(x)$ which is formed by the convolution of $\mathcal{N}_\lambda(x)$ and $p(x)$

$$p_\lambda(x) = \int_{-\infty}^{\infty} \mathcal{N}_\lambda(x-u)p(u)d(u) \quad (3)$$

converges uniformly to $p(x)$ on every interior sub-interval of $(-\infty, \infty)$.

This Lemma is a restatement of Theorem 2.1 in [54]. The implication of this Lemma is that priors for images, videos, light-fields and other visual signals can all be approximated using a GMM prior with appropriate number of mixture components, thereby allowing our framework to be applied to analyze a wide range of computational imaging systems.

- **Analytical Tractability:** Unlike other state-of-the-art signal priors such as dictionary learning [4], [40] and BM3D [14], we can analytically compute a good lower bound on MMSE [19] as described in section 9.

3.4 Performance Characterization

We characterize the performance of multiplexed imaging systems under (a) the noise model described in section 3.2 and (b) the scene prior model described in section 3.3. For a given multiplexing matrix H , we will study two metrics of interest: (1) $mmse(H)$, which is the minimum mean squared error (MMSE) and (2) multiplexing SNR gain $G(H)$ defined as the SNR gain (in dB) of the multiplexed system H over that of the impulse imaging system whose H -matrix is the identity matrix I :

$$G(H) = 10 \log_{10} \left(\frac{mmse(I)}{mmse(H)} \right). \quad (4)$$

4 ANALYTIC PERFORMANCE CHARACTERIZATION OF CI SYSTEMS USING GMM PRIOR

Mean Squared Error (MSE) is a common metric for characterizing the performance of linear systems under Bayesian setting. Among all estimators the MMSE estimator achieves the minimal MSE and we use the corresponding error (MMSE) for characterizing the performance of the CI systems. As discussed earlier in Section 3, we model the signal using GMM prior and the noise using Gaussian distribution and compute the MMSE of the CI systems. Recently, Flam et al. [19] have derived the MMSE estimator and the corresponding error (MMSE) for linear systems under GMM signal prior and GMM noise model. Ours is thus a special case with the noise being Gaussian distributed, see section 3.2. We present the expressions of the MMSE estimator and the corresponding error here, for derivations see [19].

GMM distribution is specified by the number of Gaussian mixture components K , the probability of each mixture component p_k , and the mean and covariance matrix $(u_x^{(k)}, C_{xx}^{(k)})$ of each Gaussian:

$$f(x) = \sum_{k=1}^K p_k \mathcal{N}(u_x^{(k)}, C_{xx}^{(k)}). \quad (5)$$

As discussed in section 3.2, we model the signal independent and dependent noise as a Gaussian distributed $\mathcal{N}(0, C_{nn})$, see Eqn. (2). From Eqn. (1), the likelihood distribution of the measurement y is given by $f(y|x) = \mathcal{N}(Hx, C_{nn})$. After applying Bayes rule, the posterior distribution $f(x|y)$ is also a GMM distribution with new weights $\alpha^{(k)}(y)$ and new Gaussian distributions $f^{(k)}(x|y)$:

$$f(x|y) = \sum_{k=1}^K \alpha^{(k)}(y) f^{(k)}(x|y), \quad (6)$$

where $f^{(k)}(x|y)$ is the posterior distribution of the k^{th} Gaussian

$$f^{(k)}(x|y) = \mathcal{N}(u_{x|y}^{(k)}(y), C_{x|y}^{(k)}) \quad (7)$$

with mean

$$u_{x|y}^{(k)}(y) = u_x^{(k)} + C_{xx}^{(k)} H^T (H C_{xx}^{(k)} H^T + C_{nn})^{-1} (y - H u_x^{(k)}), \quad (8)$$

and covariance matrix

$$C_{x|y}^{(k)} = C_{xx}^{(k)} - C_{xx}^{(k)} H^T (H C_{xx}^{(k)} H^T + C_{nn})^{-1} H C_{xx}^{(k)}. \quad (9)$$

The new weights $\alpha^{(k)}(y)$ are the old weights p_k modified by the probability of y belonging to the k^{th} Gaussian mixture component

$$\alpha^{(k)}(y) = \frac{p_k f^{(k)}(y)}{\sum_{i=1}^K p_i f^{(i)}(y)}, \quad (10)$$

where $f^{(k)}(y)$, which is the probability of y belonging to the k^{th} Gaussian component, is given by:

$$f^{(k)}(y) = \mathcal{N}(y; H u_x^{(k)}, H C_{xx}^{(k)} H^T + C_{nn}) \quad (11)$$

The MMSE estimator $\hat{x}(y)$ is the mean of the posterior distribution $f(x|y)$, i.e.,

$$\hat{x}(y) = \sum_{k=1}^K \alpha^{(k)}(y) u_{x|y}^{(k)}(y). \quad (12)$$

The corresponding MMSE is given by

$$mmse(H) = E \|x - \hat{x}(y)\|^2 \quad (13)$$

As shown in [19] (see Eqns. 26-29 in [19]), the $mmse(H)$ can be written as a sum of two terms: an *intra-component* error term and an *inter-component* error term.

$$mmse(H) = \sum_{k=1}^K p_k Tr(C_{x|y}^{(k)}) + \sum_{k=1}^K p_k \int_y \|\hat{x}(y) - u_{x|y}^{(k)}(y)\|^2 f^{(k)}(y) dy, \quad (14)$$

where Tr denotes matrix trace. Any given observation y is sampled from one of the K Gaussian mixture components. The first term in Eqn. (14) is the intra-component error, which is the MSE for the case when y has been correctly identified with its original mixture component. The second term is the inter-component error, which is the MSE due to inter-component confusion. The proof for the above decomposition is given in [19]. Note that the first term in Eqn. (14) is independent of the observation y and depends only on the multiplexing matrix H , the noise covariance C_{nn} , and the learned GMM prior parameters p_k , and C_{xx} and can be computed analytically. However, we need Monte-Carlo simulations to compute the second term in Eqn. (14).

5 COMMON FRAMEWORK FOR ANALYSIS OF CI SYSTEMS

We study the performance of various CI systems under the practical consideration of illumination conditions and sensor characteristics.

5.1 Performance Characterization

Computational Imaging (CI) systems improve upon traditional imaging systems by allowing more light to be captured by the sensor. However, captured images then require decoding, which typically results in noise amplification. To improve upon performance, the benefit of increased light throughput needs to outweigh the degradations caused by the decoding process. The combined effect of these two processes is measured as the SNR gain. Following the approach of [12], we measure SNR gain relative to impulse imaging. However, the analysis in [12] does not address the fact that impulse imaging performance can be significantly improved upon by state of the art image denoising methods [14], [8], [36]. We correct this by denoising our impulse images using the GMM prior. The effect this has on performance is clearly seen in Figure 1. The dotted blue line

corresponds to impulse imaging without denoising, while the solid blue line corresponds to impulse imaging after denoising using the GMM prior. Thus, the results presented in Figures 2, 4 show the performance improvements obtained due to CI over that of impulse imaging with state of the art denoising. Another important result of this paper, is that much like [8], [36], we are also able to quantify the significant performance improvements that can be obtained through image denoising.

5.2 Scene Illumination Level

The primary variable that controls the SNR of impulse imaging is the scene illumination level. As discussed in section 3.2, we consider two noise types: photon noise (signal dependent) and read noise (signal independent). Photon noise is directly proportional to the scene illumination level, whereas, read noise is independent of it. At low illumination levels, read noise dominates the photon noise but, since signal power is low, the SNR is typically low. At high scene illumination levels, photon noise dominates the read noise. Recognizing this, we compare CI techniques to impulse imaging over a wide range of scene illumination levels.

5.3 Imaging System Specification

Given the scene illumination level I_{src} (in lux), the average scene reflectivity (R) and the camera parameters such as the f-number ($F/\#$), exposure time (t), sensor quantum efficiency (q), and pixel size (δ), the average signal level in photo-electrons (J) of the impulse camera is given by [12]¹:

$$J = 10^{15} (F/\#)^{-2} t I_{src} R q (\delta)^2. \quad (15)$$

In our experiments, we assume an average scene reflectivity of $R = 0.5$ and sensor quantum efficiency of $q = 0.5$, aperture setting of $F/11$ and exposure time of $t = 6$ milliseconds, which are typical settings in consumer photography.

Sensor characteristics impact the SNR directly: sensors with larger pixels produce a higher SNR at the same scene illumination level. Here, we choose three different example cameras that span the a wide range of consumer imaging devices: 1) a high end SLR camera, 2) a machine vision camera (MVC) and 3) a smartphone camera (SPC). For each of these example camera types, we choose parameters that are typical in the marketplace today: sensor pixel size: $\delta_{SLR} = 8\mu m$ for the SLR camera, $\delta_{MVC} = 2.5\mu m$ for the MVC, and $\delta_{SPC} = 1\mu m$ for the SPC. We also assume a sensor read noise of $\sigma_r = 4e^-$ which is typical for today's CMOS sensors. The x-axis of the plots shown in Figures 1, 2 and 4 for SLR, MVC and the SPC are simply shifted relative to one another.

5.4 Experimental Details

The details of the experimental setup are as follows

- **Learning:** We learn GMM patch priors from a large collection of training patches. For EDOF and motion

1. The signal level will be larger for CI techniques. The increase in signal is encoded in the multiplexing matrix H , as discussed in Section 4

deblurring experiments, we learn the prior model using the 200 training images from Berkeley segmentation dataset [41]. For LF experiment, we use the Stanford light field dataset ² for learning the prior model. For learning we use a variant of the Expectation Maximization approach to ascertain the model parameters. We also test that the learned model is an adequate approximation of the real image prior by performing rigorous statistical analysis and comparing performance of the learned prior with state of the art image denoising methods [14]. Since, we learn GMM prior on image patches, patch size is an important parameter that needs to be chosen carefully. We choose patch size based on two considerations: 1) patch size should be bigger than the size of local multiplexing (blur kernel size) and 2) it is difficult to learn good prior for large patch sizes. In the analysis of EDOF systems, we have chosen blur kernel of 11×11 for focal sweep [31], coded aperture by Zhou et al. [65] and coded aperture by Levin et al. [33]. We experimented with different patch sizes ($> 11 \times 11$) and found that patch size of 24×24 gives the best simulation results. Thus, for our experiments on EDOF systems, we chose the patch size to be 24×24 . In the analysis of motion deblurring systems, we have chosen the flutter shutter kernel size to be 1×33 and motion invariant kernel size to be 1×9 . After experimenting with different GMM patch sizes ($> 1 \times 33$), we found that patch size of 4×256 gives the best simulation results and hence we chose that patch size for analysis of motion deblurring systems. For LF experiment we use GMM patch prior of size $16 \times 16 \times 5 \times 5$ as proposed in [43]. Further in-depth study is required for optimal choice of patch sizes for each application. However, this is outside the scope of this paper and is a topic of focus for future study.

- **Analytic Performance metric:** Analytic performance is compared using the MMSE metric. Once the MMSE is computed for the impulse and CI systems, we compute the multiplexing SNR gain in dB using Eqn. (4). The analytic multiplexing gain for various CI systems are shown in Figures 1, 2 and 4(a).

- **Analytic Performance without Prior:** To calculate the performance of CI systems without signal priors taken into account, we compute the MSE as:

$$mse(H) = Tr(H^{-1}C_{nn}H^{-T}), \quad (16)$$

where H is the corresponding multiplexing matrix and C_{nn} is the noise covariance matrix.

- **Analytic Performance with Prior:** The analytic performance of CI systems with priors taken into account is computed as described in Section 4 (Eqn. (14)). These results are shown in Figures 1, 2 and 4(a).

- **Simulations Results for Comparison:** In order to validate our analytic predictions, we also performed

2. <http://lightfield.stanford.edu/lfs.html>

extensive simulations. In our simulations, we used the MMSE estimator, Eqn. (12), to reconstruct the original (sharp) images. The MMSE estimator has been shown to provide state of art results for image denoising [36], and here we extend these powerful methods for general demultiplexing. For comparison we also perform simulations using BM3D [14]. For EDOF and motion deblurring simulations we use the image deblurring version of the BM3D algorithm [15], and for light field simulations we first perform linear reconstruction and then denoise it using the BM3D algorithm. Some images of our simulation experiments are shown in Figures 3, 5 and 7, providing visual and qualitative comparison between CI and traditional imaging techniques. The simulation results are consistent with our analytic predictions and show that CI provides performance benefits over a wide range of imaging scenarios.

6 PERFORMANCE ANALYSIS OF EDOF SYSTEMS

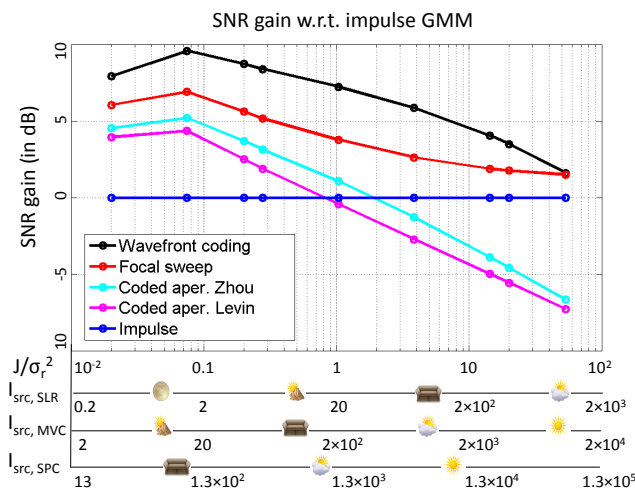


Fig. 2. *Analytic performance of EDOF systems under signal prior:* We plot the SNR gain of various EDOF systems at different photon to read noise ratios (J/σ_r^2). In the extended x-axis, we also show the effective illumination levels (in lux) required to produce the given J/σ_r^2 for the three camera specifications: SLR, MVC and SPC. The EDOF systems that we consider are: cubic phase wavefront coding [16], focal sweep camera [31], and the coded aperture designs by Zhou et al. [65] and Levin et al. [33]. Signal priors are used to improve performance for both CI and impulse cameras. Wavefront coding gives the best performance amongst the compared EDOF systems and the SNR gain varies from a significant 9.6 dB at low light conditions to 1.6 dB at high light conditions. This demonstrates the benefits of multiplexing beyond the use of signal priors, especially at low light conditions. For corresponding simulations, see figure 3.

We study the SNR gain of various EDOF systems with and without the use of signal priors. For the signal prior,

we learn a GMM patch prior of patch size 24×24 with 1500 Gaussian mixtures. First we study the performance of a particular EDOF system, focal sweep [31], and compare it with impulse imaging. We assume the aperture size of the focal sweep system to be 11×11 times bigger than that of the impulse camera, corresponding to an aperture setting of $F/1$. Hence, the light throughput of focal sweep is about 121 times that of the impulse camera. Figure 1 shows the analytical SNR gain for focal sweep and impulse cameras with and without using signal prior. The plot shows performance measured relative to impulse imaging without a signal prior (no denoising). Without signal prior, focal sweep has a huge SNR gain over impulse imaging at low photon to read noise ratio, J/σ_r^2 . This is consistent with the result obtained in [12]. However, given that most state-of-the-art reconstruction algorithms are based on signal priors, these gains are unrealistic. When the signal prior is taken into account, we get realistic gains of 7 dB at low light conditions. From the plot it is also clear that the use of prior increases SNR much more than does multiplexing.

Further, we study the performance of various other EDOF systems such as cubic phase wavefront coding [16], and the coded aperture designs by Zhou et al. [65] and Levin et al. [33]. Figure 2 shows the SNR gain (in dB) of these EDOF systems with respect to impulse imaging *under signal prior* (denoising). Amongst these systems, wavefront coding gives the best performance with SNR gain varying from a significant 9.6 dB at low light conditions to 1.6 dB at high light conditions. For corresponding simulations, see figure 3. Again from the simulations we can conclude that the use of signal prior significantly increases the performance of both impulse and CI systems and that wavefront coding gives significant performance gain over impulse imaging even after taking signal priors into account. In figure 3, we also show reconstructions using BM3D [14]. For the impulse system and coded aperture of Levin, GMM and BM3D give similar reconstruction SNR, whereas for the focal sweep and wavefront coding BM3D reconstructions are 2 dB better than the GMM reconstruction.

Practical Implications: The main conclusions of our analysis are

- *The use of signal priors improves the performance of both CI and impulse imaging significantly.*
- *Wavefront coding gives the best performance amongst the compared EDOF systems and the SNR gain varies from a significant 9.6 dB at low light conditions to 1.6 dB at high light conditions. This demonstrates the benefits of multiplexing beyond the use of signal priors, especially at low light conditions.*

3. The performance of coded aperture systems reported here is overoptimistic because we assume perfect kernel estimation, as discussed in Section 1.

4. The watch image for simulation is obtained courtesy Ivo Ihrke and Matthias B. Hullin.

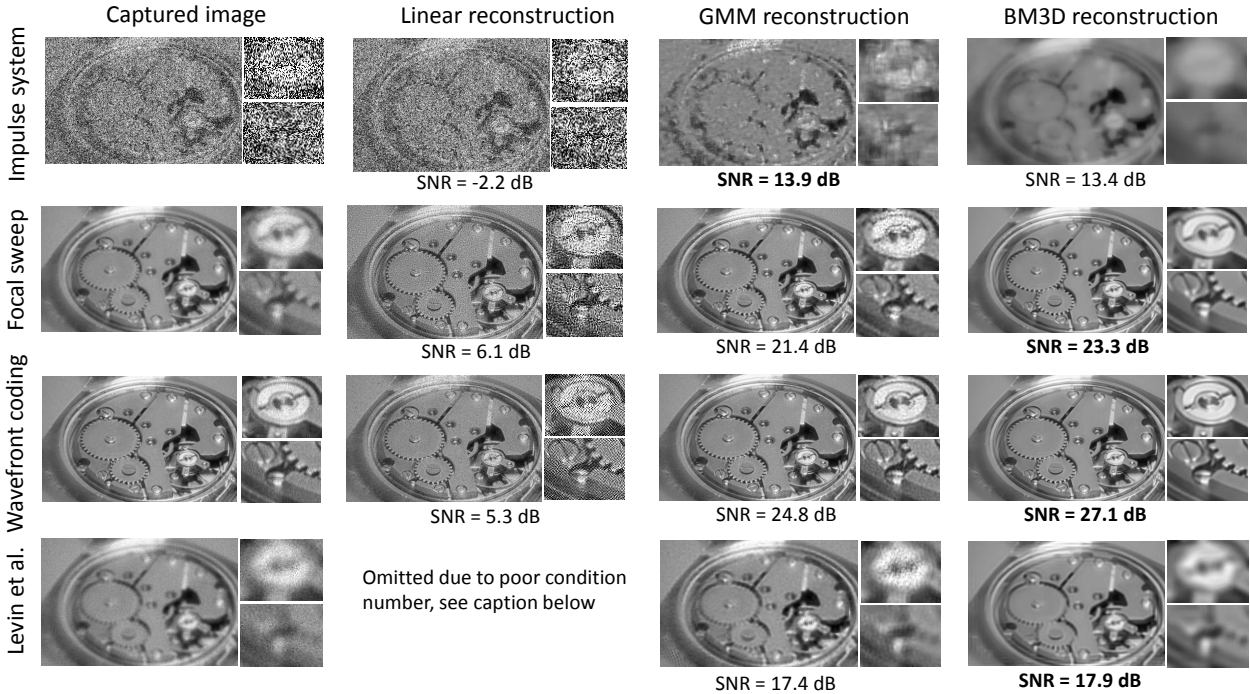


Fig. 3. *Simulation results for EDOF systems at low light condition (photon to read noise ratio of $J/\sigma^2 = 0.2$):* We show reconstruction results for many EDOF systems with and without signal prior. We do not show linear reconstruction for coded aperture design of Levin et al. [33], because the corresponding H matrix has poor condition number. The frequency spectrum of the designed code has zeroes, which are good for estimating depth from defocus but not good for reconstruction. Note that the use of signal prior significantly increases the performance of both impulse and CI systems. Using GMM prior, focal sweep [31], wavefront coding [16] and coded aperture design of Levin et al. [33] produce SNR gains (w.r.t. impulse system) of 7.5 dB, 10.9 dB and 3.5 dB respectively, which are significant gains. For impulse imaging and coded aperture of Levin, GMM and BM3D give similar reconstruction SNR, where as for the focal sweep and wavefront coding BM3D reconstructions are 2 dB better than the GMM reconstruction

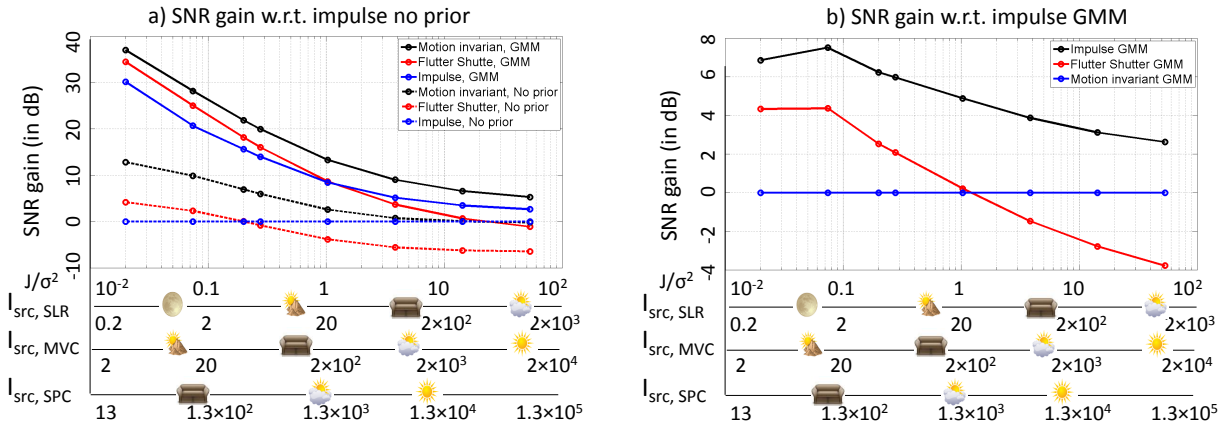


Fig. 4. *Analytic performance of motion deblurring systems:* We study the performance of motion invariant [38], flutter shutter [48] and impulse cameras with and without the use of signal priors. From subplot (a), it is clear that SNR gain due to signal prior is much more than due to multiplexing. However, after taking into account the effect of signal prior, multiplexing still produce significant SNR gains as shown in subplot (b). Motion invariant imaging produces SNR gains ranging from 7.5 dB at low light conditions to 2.5 dB at high light conditions. For corresponding simulations, see figure 5.

7 PERFORMANCE ANALYSIS OF MOTION DEBLURRING SYSTEMS

We study the performance of two motion deblurring systems: the flutter shutter [48] and motion invariant camera [38]. Again, we focus our attention on the case where

signal priors are taken into account. For this experiment, we learn a GMM patch prior, of patch size 4×256 , with 1500 Gaussian mixtures. For the motion deblurring cameras, we set the exposure time to be 33 times that of the impulse camera, corresponding to an exposure time of

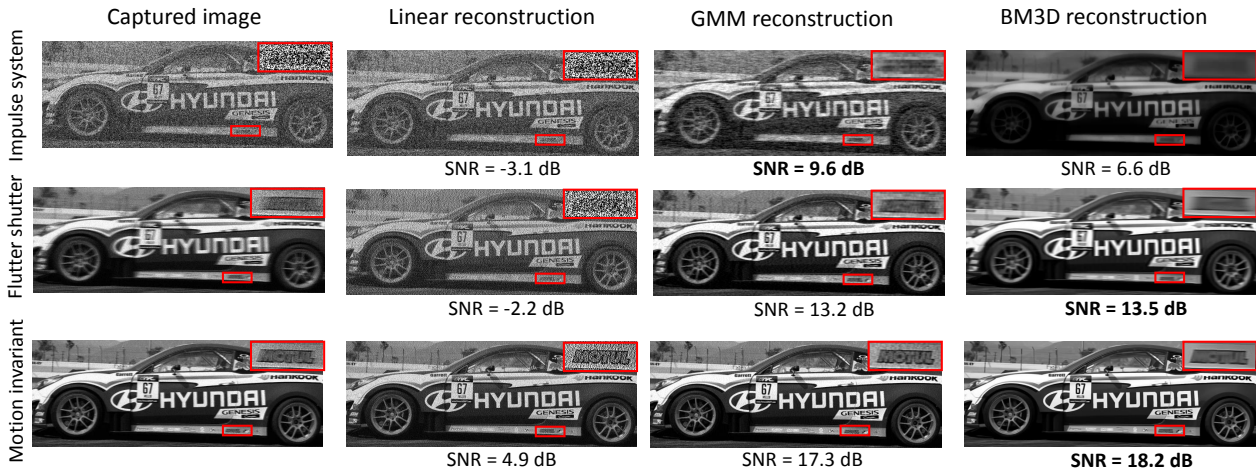


Fig. 5. Simulation results for motion deblurring systems at low light condition (photon to read noise ratio of $J/\sigma^2 = 0.2$). Using GMM prior, flutter shutter [48] and motion invariant system [38] produce SNR gains (w.r.t. impulse system) of 3.6 dB and 7.7 dB respectively. For the impulse system, GMM reconstruction is 3 dB better than the BM3D reconstruction, whereas for the flutter shutter and motion invariant system, GMM and BM3D produce similar results.

200 milliseconds. The binary flutter shutter code that we used in our experiment has 15 'ones' and hence the light throughput is 15 times that of the impulse imaging system. The light throughput of the motion invariant camera is 33 times that of the impulse camera. Figure 4(a) shows the analytic SNR gain (in dB) of the motion deblurring systems with respect to impulse imaging without signal prior⁵. Clearly, the SNR gain due to signal prior is much more than that due to multiplexing. However, after taking into account the effect of signal prior, multiplexing still produces significant SNR gain as shown in 4(b). Motion invariant imaging produces SNR gains ranging from 7.5 dB at low light conditions to 2.5 dB at high light conditions. Figure 5 shows the corresponding simulation results. At the low photon to read noise ratio of $J/\sigma_r^2 = 0.2$, motion invariant imaging performs 7.7 dB better than impulse imaging. We also show simulation results using BM3D reconstruction. For impulse system, GMM reconstruction is 3 dB better than the BM3D reconstruction, whereas for the CI systems, both the reconstructions are similar.

Practical Implications: The main conclusion of our analysis is

- Motion invariant imaging produces SNR gains ranging from 7.5 dB at low light conditions to 2.5 dB at high light conditions.

8 PERFORMANCE ANALYSIS OF LIGHT FIELD SYSTEMS

We study the performance of two light field cameras: 1) the micro-lenses array based Lytro camera [45] and 2) MURA mask based light field camera [32]. The corresponding impulse system is a pin-hole mask array placed at the micro lenses array location. We use the GMM patch prior of size $16 \times 16 \times 5 \times 5$ as proposed in [43], which learns a Gaussian

5. Flutter shutter performance reported here is overoptimistic because we assume perfect kernel estimation, as discussed in Section 1.

component for each disparity value between the LF views. In our experiment we chose 11 disparity values ranging from $-5 : 5$ and thus we learn GMM with 11 components. For the MURA mask based LF we use tiled MURA mask with the basic tile of size 5×5 . The multiplexing matrix H corresponding to the pin-hole mask array LF is the identity matrix, whereas the multiplexing matrix of Lytro is a scaled version of identity with the scale (light throughput) given by the ratio of the lenselet area to the pinhole area. For MURA based LF, the captured 2-D multiplexed image is obtained by inner product between the 5×5 angular dimension of the LF and cyclically shifted versions of the basic 5×5 MURA mask and the H matrix is constructed keeping this structure in mind. The locality of MURA-based reconstruction that enables a patch approach was established in [30]. Figure 6(a-b) shows the analytic SNR gains for the two CI systems w.r.t. the impulse system. As in the case of EDOF and motion deblurring systems, the gain due to signal prior is more than that due to multiplexing. Note that the SNR gain of Lytro is high even at high light levels. This is true for both with and without signal prior cases. This is because the multiplexing matrix of Lytro is a scaled version of the impulse multiplexing matrix. In our set-up, the light throughput of Lytro is about 20 times that of the impulse system and so it is always about 13 dB better than the impulse system. Figure 7 shows corresponding simulations. From our analysis, we conclude that Lytro provides significant SNR gain at high light levels, but similar performance to MURA at low light levels. However, we should keep in mind that the systems analyzed here all trade-off the spatial resolution for angular resolution and hence capture low spatial resolution light field data. There are designs that capture full spatial resolution light field data [42], but we have not analyzed them as the scope of this paper is limited to analyzing fully-determined systems for which we can define a corresponding impulse system.

Practical Implications: The main conclusion of our anal-

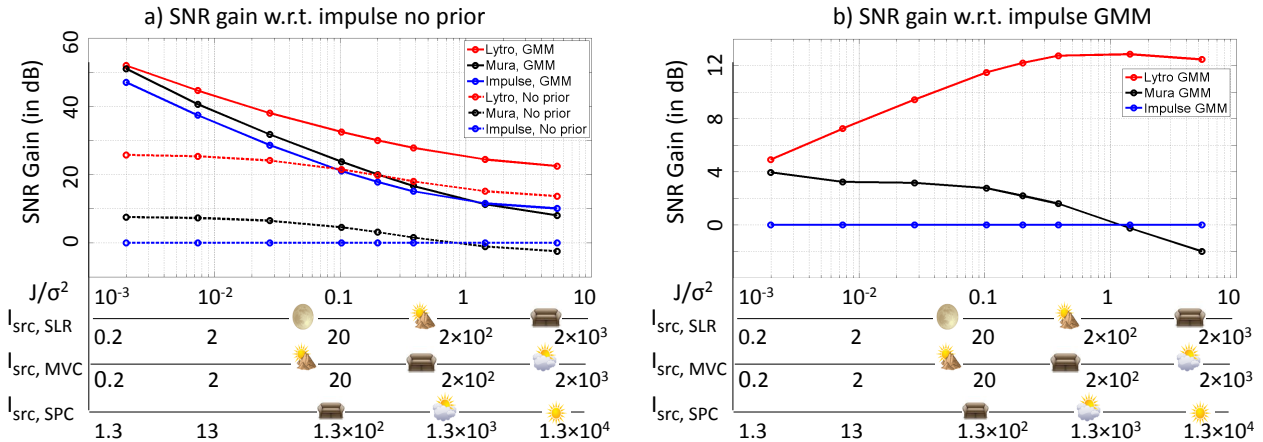


Fig. 6. *Analytic performance of light field cameras:* We study the performance of the micro-lenses array based Lytro camera [45] and MURA mask based light field camera [32] against the light field impulse system (a pin-hole array mask camera). As in the case of EDOF and motion deblurring systems, the gain due to signal prior is much more than that due to multiplexing. Note that the SNR gain (w.r.t. impulse system) for Lytro is high even at high light levels. This is true for both with and without signal prior cases. This is because the multiplexing matrix of Lytro is a scaled version of the impulse multiplexing matrix, where the scale (light throughput) is given by the ratio of the lenselet area to the pinhole area. In our set-up, the light throughput of Lytro is about 20 times that of the impulse system and so it is always about 13 dB better than the impulse system. For corresponding simulations, see Figure 7.

ysis is

- *Lytro provides significant SNR gain at high light levels, but similar performance to MURA at low light levels.*

9 EXACT MMSE VS. ITS LOWER AND UPPER BOUNDS

The exact expression for MMSE is given by Eqn. (14). As discussed in section 4, the first term depends only on the multiplexing matrix H , the noise covariance C_{nn} , and the learned GMM prior parameters p_k and C_{xx} and can be computed analytically. But we need to perform Monte-Carlo simulations to compute the second term. However, we can use the analytic first term as a lower bound on MMSE (and hence upper bound on SNR), i.e.,

$$mmse(H) \geq \sum_{k=1}^K p_k Tr(C_{x|y}^{(k)}). \quad (17)$$

Flam et al. [19] have also provided an upper bound for the MMSE, see Theorem 1 in [19]. They have shown that the LMMSE (linear MMSE) estimation error is an upper bound of the MMSE error. The LMMSE estimation error $lmmse$ is given by:

$$lmmse(H) = Tr(C_{xx} - C_{xx} H^T (H C_{xx} H^T + C_{nn})^{-1} H C_{xx}), \quad (18)$$

where

$$C_{xx} = \sum_{k=1}^K p_k (C_{xx}^{(k)} + u_x^{(k)} u_x^{(k)T}) - u_x u_x^T$$

$$u_x = \sum_{k=1}^K p_k u_x^{(k)}.$$

We compare the exact MMSE with its analytic lower and upper bounds given by Eqn. (17) and Eqn. (18), respectively, for the EDOF and motion deblurring systems. Figure 8(a) shows that, for the wavefront coding system, the lower bound is a very good approximation for the MMSE over the range $0.01 \leq J/\sigma^2 \leq 100$. We do not show the corresponding plots for other EDOF systems as they are very similar to the wavefront coding system. Figure 8(b) shows that the same conclusion holds for motion invariant system. Note that though for these systems the lower bound is a very good approximation of the MMSE over the shown illumination range, it does not mean that this holds true for all light levels or for all systems. There are three factors which determine how well the lower bound can approximate the MMSE: 1) the multiplexing system H (fully determined H matrices are less likely to produce inter-component error as compared to under-determined systems), 2) noise level (large noise will lead to more inter-component error) and 3) location of Gaussian components in the GMM prior model.

From the above experiment, we conclude that we can use the analytic lower bound expression for computing the MMSE of many EDOF and motion deblurring systems over a wide range of lighting condition. This also suggests that we can use the analytic lower bound expression of MMSE, Eqn. (17), for solving the optimal CI design problem, i.e., finding the H that minimizes Eqn. (17), over a wide range of light levels.

10 DISCUSSIONS

We present a framework to comprehensively analyze the performance of CI systems. Our framework takes into account the effect of multiplexing, affine noise and signal priors. We model signal priors using a GMM, which can approximate almost all prior signal distributions. More

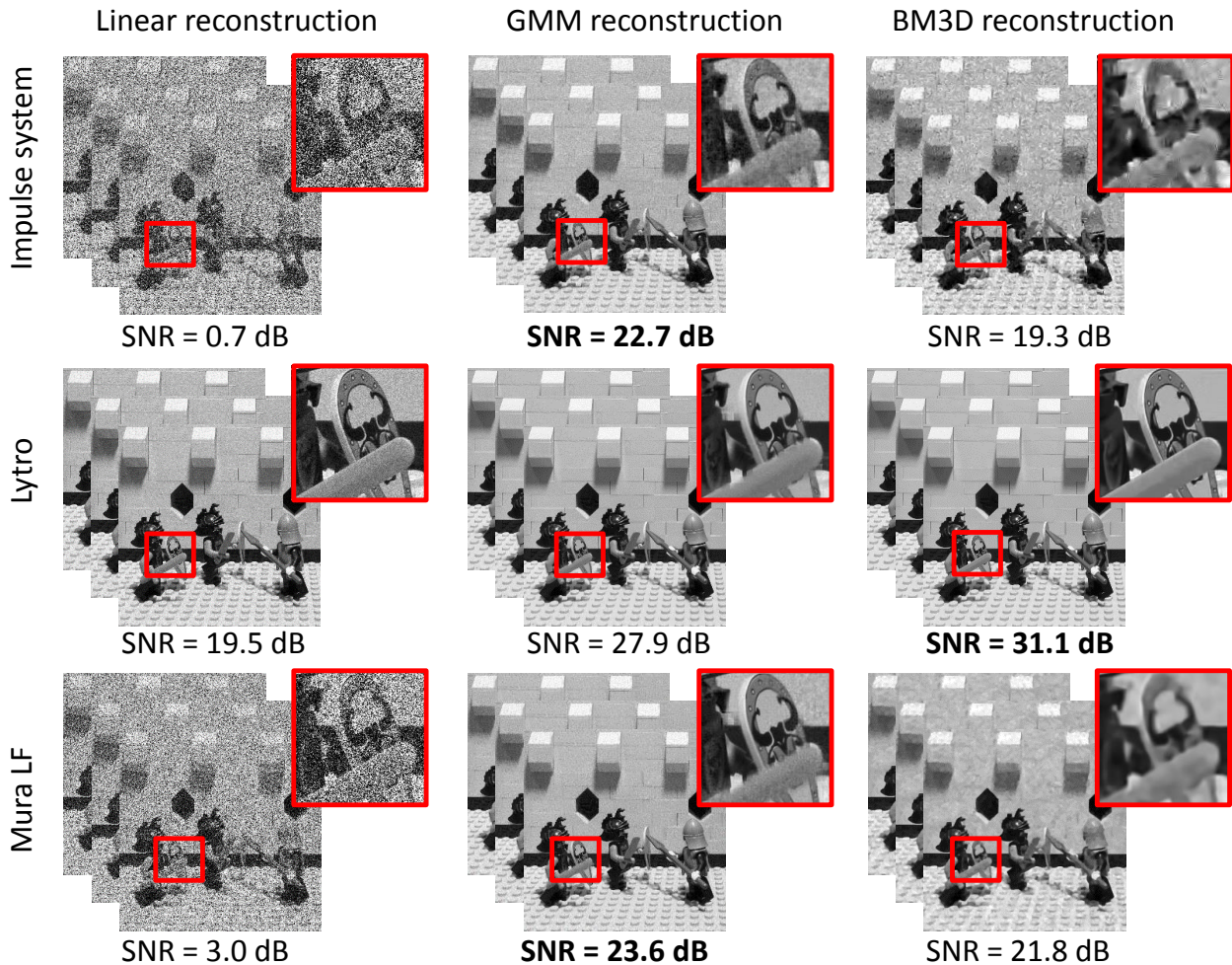


Fig. 7. Simulation results for light field cameras at low light condition (photon to read noise ratio of $J/\sigma^2 = 0.2$). Using GMM prior, Lytro [45] and MURA mask based light field camera [32] produce SNR gains (w.r.t. impulse systems) of 5.2 dB and 0.9 dB respectively.

importantly, the prior is analytically tractable. We use the MMSE metric to characterize the performance of any given linear CI system. Our analysis allows us to determine the increase in performance of CI systems *when signal priors are taken into account*. We use our framework to analyze several CI techniques, specifically, EDOF, motion deblurring and light field cameras. Our analysis reveals that: 1) Signal priors increase SNR more than multiplexing, and 2) Multiplexing gain (above and beyond that due to signal prior) is significant especially at low light conditions. Moreover, we use our framework to establish the following practical implications: 1) Amongst the EDOF systems analyzed in the paper, Wavefront coding gives the best performance with SNR gain (over impulse imaging) of 9.6 dB at low light conditions, 2) Amongst the motion deblurring systems, motion invariant system provides the best performance with SNR gain of 7.5 dB at low light conditions, and 3) Lytro provides the best performance amongst compared light field systems with SNR gain of 12 dB at high light conditions.

While the results reported in this paper are specific to EDOF, motion deblurring and light field cameras, the

framework can be applied to analyze any linear CI camera. In the future, we would like to use our framework to learn priors and analyze multiplexing performance for other types of datasets (e.g. videos, hyperspectral volumes, reflectance fields). Of particular interest is the analysis of compressive CI techniques. Analyzing the performance of compressed sensing matrices has been a notoriously difficult problem, except in a few special cases (e.g. Gaussian, Bernoulli, and Fourier matrices). Our framework can gracefully handle any arbitrary multiplexing matrix, and thus could prove to be a significant contribution to the compressed sensing community. By the same token, we would like to apply our analysis to overdetermined systems so that we may also analyze multiple image capture CI techniques (e.g. Hasinoff et al. [25] and Zhang et al. [63]). Finally, and perhaps most significantly, we would like to apply our framework towards the problem of parameter optimization for different CI techniques. For instance, we may use our framework to determine the optimal aperture size for focal sweep cameras, the optimal flutter shutter code for motion deblurring, or the optimal measurement matrix for a compressed sensing system. In this way, we believe our

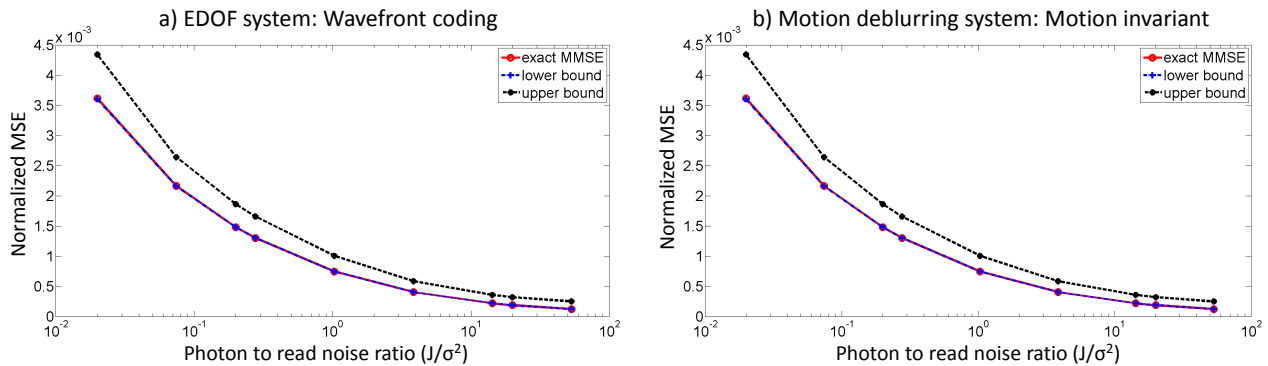


Fig. 8. *Exact MMSE vs. its lower and upper bounds*: We compare the exact MMSE with its analytic lower bound given by Eqn. (17) and upper bound given by Eqn. (18). Subplot (a) shows that, for the wavefront coding system, the lower bound is a very good approximation for the MMSE over the range $0.01 \leq J/\sigma^2 \leq 100$. We do not show the corresponding plots for other EDOF systems as they are very similar to the wavefront coding system. Subplot (b) shows that the same conclusion holds for motion invariant system (and flutter shutter, not shown here). Thus, we can use the analytic lower bound for MMSE for both analysis and design of CI systems over a wide range of lighting levels.

framework can be used to exhaustively analyze the field of CI research and provide invaluable answers to existing open questions in the field.

11 ACKNOWLEDGEMENTS

Kaushik Mitra and Ashok Veeraraghavan acknowledge support through NSF Grants NSF-IIS: 1116718, NSF-CCF:1117939 and a research grant from Samsung Advanced Institute of Technology through the Samsung GRO program.

REFERENCES

- [1] A. Agrawal, M. Gupta, A. Veeraraghavan, and S. Narasimhan. Optimal coded sampling for temporal super-resolution. In *IEEE Conference on Computer Vision and Pattern Recognition (CVPR)*, 2010. 2
- [2] A. Agrawal and R. Raskar. Optimal single image capture for motion deblurring. In *CVPR*, 2009. 3
- [3] A. Agrawal, A. Veeraraghavan, and R. Raskar. Reinterpretable imager: Towards variable post capture space, angle and time resolution in photography. 29, 2010. 2
- [4] M. Aharon, M. Elad, and A. Bruckstein. k-svd: An algorithm for designing overcomplete dictionaries for sparse representation. *IEEE Transactions on Signal Processing*, 54(11):4311–4322, 2006. 2, 4
- [5] J. Baek. Transfer Efficiency and Depth Invariance in Computational Cameras. In *ICCP*, 2010. 3
- [6] R. Baer, W. Holland, J. Holm, and P. Vora. A comparison of primary and complementary color filters for ccd-based digital photography. In *SPIE Electronic Imaging Conference*. Citeseer, 1999. 2
- [7] A. Castro and J. Ojeda-Castañeda. Asymmetric phase masks for extended depth of field. *Appl. Opt.*, 43(17):3474–3479, Jun 2004. 2
- [8] P. Chatterjee and P. Milanfar. Is denoising dead? *Image Processing, IEEE Transactions on*, 19(4):895–911, 2010. 3, 5, 6
- [9] M. Chen, J. Silva, J. Paisley, C. Wang, D. Dunson, and L. Carin. Compressive sensing on manifolds using a nonparametric mixture of factor analyzers: Algorithm and performance bounds. *IEEE Transactions on Signal Processing*, 58(12):61406155, December 2010. 4
- [10] T. Cho, A. Levin, F. Durand, and W. Freeman. Motion blur removal with orthogonal parabolic exposures. In *ICCP*, 2010. 2, 3
- [11] O. Cossairt. Tradeoffs and Limits in Computational Imaging (Ph.D. Thesis). Technical report, Sep 2011. 2, 3
- [12] O. Cossairt, M. Gupta, and S. K. Nayar. When does computational imaging improve performance? *IEEE transactions on image processing*, 22(1-2):447–458, 2013. 1, 2, 3, 5, 6, 7
- [13] O. Cossairt, C. Zhou, and S. K. Nayar. Diffusion Coding Photography for Extended Depth of Field. In *SIGGRAPH*, 2010. 3
- [14] K. Dabov, A. Foi, V. Katkovnik, and K. Egiazarian. Image denoising by sparse 3-d transform-domain collaborative filtering. *TIP*, 16(8), 2007. 2, 4, 5, 6, 7
- [15] K. Dabov, A. Foi, V. Katkovnik, and K. Egiazarian. Image restoration by sparse 3d transform-domain collaborative filtering. In *SPIE Electronic Imaging*, 2008. 7
- [16] E. Dowski Jr and W. Cathey. Extended depth of field through wavefront coding. *Applied Optics*, 34(11):1859–1866, 1995. 2, 7, 8
- [17] Y. C. Eldar, P. Kuppinger, and H. Bolcskei. Block-sparse signals: Uncertainty relations and efficient recovery. *IEEE Transactions on Signal Processing*, 58(6):30423054, November 2010. 4
- [18] Y. C. Eldar and M. Mishali. Robust recovery of signals from a structured union of subspaces. *IEEE Transactions on Information Theory*, 55(11):53025316, November 2009. 4
- [19] J. T. Flam, S. Chatterjee, K. Kansanen, and T. Ekman. On mmse estimation: A linear model under gaussian mixture statistics. *IEEE Transactions on Signal Processing*, 60(7), 2012. 3, 4, 5, 10
- [20] E. E. García-Guerrero, E. R. Méndez, H. M. Escamilla, T. A. Leskova, and A. A. Maradudin. Design and fabrication of random phase diffusers for extending the depth of focus. *Opt. Express*, 15(3):910–923, Feb 2007. 2
- [21] N. George and W. Chi. Extended depth of field using a logarithmic asphere. *Journal of Optics A: Pure and Applied Optics*, 2003. 2
- [22] J. A. Guerrero-Colon, L. Mancera, and J. Portilla. Image restoration using space-variant gaussian scale mixtures in overcomplete pyramids. *IEEE Transactions on Image Processing*, 17(1):2741, January 2008. 4
- [23] Q. Hanley, P. Verveer, and T. Jovin. Spectral imaging in a programmable array microscope by hadamard transform fluorescence spectroscopy. *Applied Spectroscopy*, 53(1), 1999. 2
- [24] M. Harwit and N. Sloane. Hadamard transform optics. *New York: Academic Press*, 1979. 2, 3
- [25] S. Hasinoff, K. Kutulakos, F. Durand, and W. Freeman. Time-constrained photography. In *ICCV*, pages 1–8, 2009. 2, 3, 4, 11
- [26] S. W. Hasinoff, K. N. K. F. Durand, and W. T. Freeman. Light-efficient photography. In *ECCV*, 2008. 2
- [27] G. Häusler. A method to increase the depth of focus by two step image processing. *Optics Communications*, 1972. 2
- [28] Y. Hitomi, J. Gu, M. Gupta, T. Mitsunaga, S. Nayar, T. Kobayashi, O. Cossairt, D. Miao, S. Nayar, C. Zhou, et al. Video from a single coded exposure photograph using a learned over-complete dictionary. In *ACM Trans. on Graphics (also Proc. of ACM SIGGRAPH)*, 2010. 2
- [29] J. Holloway, A. Sankaranarayanan, A. Veeraraghavan, and S. Tambe. Flutter shutter video camera for compressive sensing of videos. In *IEEE International Conference on Computational Photography (ICCP)*, pages 1–9, 2012. 2
- [30] I. Ihrke, G. Wetzstein, and W. Heidrich. A theory of plenoptic multiplexing. In *CVPR*, 2010. 1, 2, 3, 4, 9
- [31] S. Kuthirummal, H. Nagahara, C. Zhou, and S. K. Nayar. Flexible Depth of Field Photography. In *PAMI*, 2010. 1, 2, 6, 7, 8

- [32] D. Lanman, R. Raskar, A. Agrawal, and G. Taubin. Shield fields: modeling and capturing 3d occluders. In *SIGGRAPH*, 2008. 1, 2, 9, 10, 11
- [33] A. Levin, R. Fergus, F. Durand, and W. Freeman. Image and depth from a conventional camera with a coded aperture. In *SIGGRAPH*. ACM, 2007. 2, 3, 4, 6, 7, 8
- [34] A. Levin, W. T. Freeman, and F. Durand. Understanding camera trade-offs through a bayesian analysis of light field projections. In *ECCV*, pages 88–101, 2008. 3
- [35] A. Levin, S. W. Hasinoff, P. Green, F. Durand, and W. T. Freeman. 4d frequency analysis of computational cameras for depth of field extension. *ACM Trans. Graph.*, 28(3), 2009. 2
- [36] A. Levin and B. Nadler. Natural image denoising: Optimality and inherent bounds. In *CVPR*, pages 2833–2840, 2011. 3, 5, 6, 7
- [37] A. Levin, B. Nadler, F. Durand, and W. T. Freeman. Patch complexity, finite pixel correlations and optimal denoising. In *ECCV* (5), pages 73–86, 2012. 3
- [38] A. Levin, P. Sand, T. Cho, F. Durand, and W. Freeman. Motion-invariant photography. In *SIGGRAPH*, 2008. 2, 3, 8, 9
- [39] C. Liang, T. Lin, B. Wong, C. Liu, and H. Chen. Programmable aperture photography: multiplexed light field acquisition. In *SIGGRAPH*, 2008. 1, 2
- [40] J. Mairal, F. Bach, J. Ponce, and G. Sapiro. Online learning for matrix factorization and sparse coding. *Journal of Machine Learning Research*, 11:19–60, 2010. 4
- [41] D. Martin, C. Fowlkes, D. Tal, and J. Malik. A database of human segmented natural images and its application to evaluating segmentation algorithms and measuring ecological statistics. In *IEEE International Conference on Computer Vision*, volume 2, pages 416–423, July 2001. 6
- [42] K. Marwah, G. Wetzstein, Y. Bando, and R. Raskar. Compressive light field photography using overcomplete dictionaries and optimized projections. *ACM Trans. Graph.*, 32(4):46, 2013. 9
- [43] K. Mitra and A. Veeraraghavan. Light field denoising, light field superresolution and stereo camera based refocusing using a gmm light field patch prior. In *CVPR Workshops*, 2012. 2, 4, 6, 9
- [44] S. Nayar. Computational camera: Approaches, benefits and limits. Technical report, DTIC Document, 2011. 1
- [45] R. Ng, M. Levoy, M. Brédif, G. Duval, M. Horowitz, and P. Hanrahan. Light field photography with a hand-held plenoptic camera. *Computer Science Technical Report*, 2, 2005. 1, 2, 9, 10, 11
- [46] J. Ojeda-Castaneda, J. E. A. Landgrave, and H. M. Escamilla. Annular phase-only mask for high focal depth. *Optics Letters*, 2005. 2
- [47] K. N. Plataniotis and D. Hatzinakos. Gaussian mixtures and their applications to signal processing. *Advanced Signal Processing: Theory and Implementation for Radar, Sonar and Medical Imaging Systems Handbook*, S. Stergiopoulos, Editor, CRC Press, pages 3.2 – 3.32, December 2000. 2, 4
- [48] R. Raskar, A. Agrawal, and J. Tumblin. Coded exposure photography: motion deblurring using fluttered shutter. In *SIGGRAPH*, 2006. 2, 3, 4, 8, 9
- [49] N. Ratner and Y. Schechner. Illumination multiplexing within fundamental limits. In *CVPR*, 2007. 1, 2, 3
- [50] N. Ratner, Y. Schechner, and F. Goldberg. Optimal multiplexed sensing: bounds, conditions and a graph theory link. *Optics Express*, 15, 2007. 3
- [51] D. Reddy, A. Veeraraghavan, and R. Chellappa. P2C2: programmable pixel compressive camera for high speed imaging. In *IEEE International Conference On Computer Vision and Pattern Recognition*, pages 329–336, 2011. 2
- [52] Y. Schechner, S. Nayar, and P. Belhumeur. Multiplexing for optimal lighting. *Pattern Analysis and Machine Intelligence, IEEE Transactions on*, 29(8):1339–1354, 2007. 2, 4
- [53] N. Shroff, A. Veeraraghavan, Y. Taguchi, O. Tuzel, A. Agrawal, and R. Chellappa. Variable focus video: Reconstructing depth and video for dynamic scenes. In *IEEE International Conference on Computational Photography (ICCP)*, pages 1–9, 2012. 2
- [54] H. W. Sorenson and D. L. Alspach. Recursive bayesian estimation using gaussian sums. *Automatica*, 7:465–479, 1971. 2, 4
- [55] Y. Tendo. Mathematical theory of the flutter shutter. *PhD. Thesis, ENS Cachan*, 2012. 3
- [56] A. Veeraraghavan, R. Raskar, A. Agrawal, A. Mohan, and J. Tumblin. Dappled photography: Mask enhanced cameras for heterodyned light fields and coded aperture refocusing. *SIGGRAPH*, 2007. 1, 2, 3, 4
- [57] A. Veeraraghavan, D. Reddy, and R. Raskar. Coded Stroboscopic Photography: Compressive Sensing of High Speed Periodic Videos. *IEEE Transactions on Pattern Analysis and Machine Intelligence*, 33(4):671–686, 2011. 2
- [58] A. Wagadarikar, R. John, R. Willett, and D. Brady. Single disperser design for coded aperture snapshot spectral imaging. *Applied Optics*, 47(10):B44–B51, 2008. 2, 3, 4
- [59] B. Wilburn, N. Joshi, V. Vaish, E. V. Talvala, E. Antunez, A. Barth, and M. Levoy. High performance imaging using large camera arrays. *ACM Transactions on Graphics (TOG)*, 24:765–776, 2005. 2
- [60] A. Wuttig. Optimal transformations for optical multiplex measurements in the presence of photon noise. *Applied Optics*, 44, 2005. 2, 3
- [61] J. Yang, X. Yuan, X. Liao, P. Llull, D. J. Brady, G. Sapiro, and L. Carin. Video compressive sensing using gaussian mixture models. 2013. 4
- [62] G. Yu, G. Sapiro, and S. Mallat. Solving inverse problems with piecewise linear estimators: From gaussian mixture models to structured sparsity. *IEEE Transactions on Image Processing*, (5), 2012. 2, 4
- [63] L. Zhang, A. Deshpande, and X. Chen. Denoising versus Deblurring: HDR techniques using moving cameras. In *CVPR*, 2010. 3, 11
- [64] C. Zhou, D. Miao, and S. Nayar. Focal Sweep Camera for Space-Time Refocusing. Technical report, Nov 2012. 2
- [65] C. Zhou and S. Nayar. What are Good Apertures for Defocus Deblurring? In *ICCP*, 2009. 2, 3, 6, 7



Kaushik Mitra is currently a postdoctoral research associate in the Electrical and Computer Engineering department of Rice University. His research interests are in computational imaging, computer vision and statistical signal processing. He earned his Ph.D. in Electrical and Computer Engineering from the University of Maryland, College Park, where his research focus was on the development of statistical models and optimization algorithms for computer vision problems



Oliver Cossairt is an Assistant Professor at Northwestern University. His research interests lie at the intersection of optics, computer vision, and computer graphics. He earned his PhD. in Computer Science from Columbia University, where his research focused on the design and analysis of computational imaging systems. He earned his M.S. from the MIT Media Lab, where his research focused on holography and computational displays. Oliver was awarded a NSF Graduate Research Fellowship, Best Paper Award at ICCP 2010, and his research was featured in the March 2011 issue of Scientific American Magazine. Oliver has authored ten patents on various topics in computational imaging and displays.



Ashok Veeraraghavan is currently an Assistant Professor of Electrical and Computer Engineering at Rice University, Tx, USA. At Rice University, Prof. Veeraraghavan directs the Computational Imaging and Vision Lab. His research interests are broadly in the areas of computational imaging, computer vision and robotics. Before joining Rice University, he spent three wonderful and fun-filled years as a Research Scientist at Mitsubishi Electric Research Labs in Cambridge, MA.

He received his Bachelor's in Electrical Engineering from the Indian Institute of Technology, Madras in 2002 and M.S and Ph.D. degrees from the Department of Electrical and Computer Engineering at the University of Maryland, College Park in 2004 and 2008 respectively. His thesis received the Doctoral Dissertation award from the Department of Electrical and Computer Engineering at the University of Maryland.